Nano Energy 53 (2018) 863–870

Contents lists available at ScienceDirect

Nano Energy

journal homepage: www.elsevier.com/locate/nanoen

Full paper

A liquid metal-based triboelectric nanogenerator as stretchable electronics for safeguarding and self-powered mechanosensing

Sheng Wang[a], Li Ding[a], Xiwen Fan[a], Wanquan Jiang[b,*], Xinglong Gong[a,*]

[a] CAS Key Laboratory of Mechanical Behavior and Design of Materials, Department of Modern Mechanics, USTC, Hefei 230027, PR China
[b] Department of Chemistry, University of Science and Technology of China (USTC), Hefei 230026, PR China

ARTICLE INFO

Keywords:
Triboelectric performance
Shear stiffening gel
Liquid metal
Safeguarding
Self-powered sensing

ABSTRACT

In recent years, high performance triboelectric nanogenerator (TENG) shows distinguished energy-harvesting property which guarantees its potential applications as a power source. However, collision and harsh impact, occurred in daily life, always injure human beings. Developing novel multifunctional TENG with self-powered mechanosensing and protection properties from violent impact is an urgent and meaningful work. Here, a multifunctional TENG with energy-harvesting, safeguarding and self-powered force-sensing properties was fabricated by assembling shear stiffening gel/polydimethylsiloxane (SSG/PDMS) matrix with GaInSn liquid metal. Operating at 10 Hz, TENG with a size of $50 \times 50 \times 4\ mm^3$ obtains an output voltage of 35.72 V, current of 5.10 μA, and maximum output power of 182.17 μW. In addition, TENG device generates enhanced output power of 323.97 μW under tensile strain of 80%. Besides harvesting mechanical energy, TENG with fast stimuli-responsive character, has been proven as a self-powered sensor to monitor varieties of physiological movements. More importantly, the TENG device with high damping property enables to dissipate 66.43% of external impact force which provides favorable protection effect. Correspondingly, the distinguished output voltage signals can also reveal and assess different impulsive loads. This work proposes a multifunctional TENG device with energy-harvesting, and utilizing the flexible TENG for safeguarding and self-powered mechanosensing.

1. Introduction

Wearable electronics as one of the most promising technologies in next-generation artificial devices have achieved revolutionary progresses in the past decades [1,2]. They have potential applications in sensors [3], artificial skins [4], touch panel [5] and smart textile [6]. Conventionally, external power sources are always required to drive these electronics. However, the disadvantages of rigidity structures, heaviness and bulky volume of these power supplies may seriously hinder the practical applications of wearable electronics. Although several flexible solar cells, Li batteries have been developed to try to settle these problems, the frequent charging and replacing operations still remain challenges in large-scale use on human skins. An ideal strategy to overcome the inconvenience is developing novel electronics with self-powered property which can harvest energy and transform it to electric energy due to the universally available biomechanical energy from ambient environment. Since first reported by Prof. Wang, the feasible triboelectric nanogenerator (TENG) with high electronic output performance, easy fabrication and environmental friendliness proves its high efficiency in energy-harvesting in recent years [7,8].

TENG based on triboelectric effect and electrostatic induction, can successfully convert mechanical energy into electric energy which can act as a new green and sustainable power source. So far, the reported TENG are mainly assembled by polymer matrix and conductive medium with various coaxial [9] and sponge [10] structures. Besides serving as a power generator, TENG with stimuli-responsive property can also be utilized as multifunctional self-powered sensing systems including gesture monitoring [11], wind flow rate sensing [12,13] and H_2 detection [14]. Additionally, high stretchability, another important function for TENG provides more preferability in human wearable electronics since human movements often include large-scale deformations. More efforts have devoted in fabricating stretchable TENG to try to avoid failure resulting from large strain in daily life [15–19]. Especially, due to the good conductivity, high flexibility, nontoxicity and avoiding cracks under stretch, Gallium-Indium liquid metal is an ideal electrode material for stretchable TENG [20]. A novel polydimethylsiloxane (PDMS) elastomer encapsulated with liquid metal could function as capacitive sensor and triboelectric generator which the motions of finger slapping or dragging across the electrode could be differentiated by various signals [21]. A self-powered cursor based on

* Corresponding authors.
E-mail addresses: jiangwq@ustc.edu.cn (W. Jiang), gongxl@ustc.edu.cn (X. Gong).

https://doi.org/10.1016/j.nanoen.2018.09.035
Received 10 August 2018; Received in revised form 14 September 2018; Accepted 17 September 2018
Available online 20 September 2018
2211-2855/

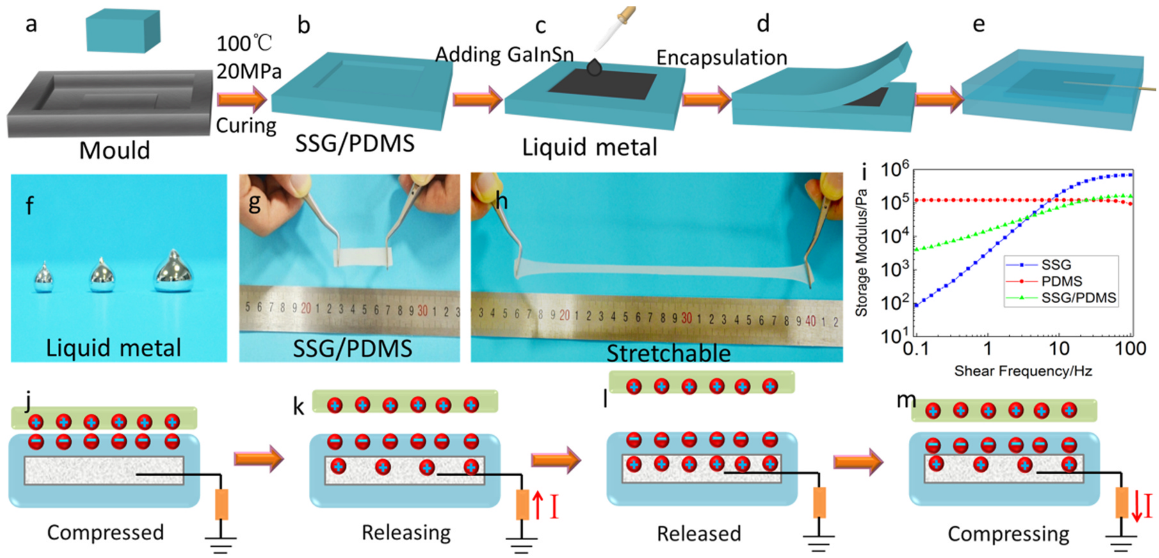

Fig. 1. Schematic diagram of the preparation process of TENG (a-e), photo of GaInSn liquid metal (f), stretchability of SSG/PDMS (g, h), rheological properties of the polymer composite (i), electricity generation process of the as-prepared TENG (j-m).

triboelectric nanogenerator was developed by injecting liquid metal into PDMS and this functional device enabled to simultaneously detect normal force and shear force direction [22]. So far, the most widely collected energy for stretchable PDMS- or Ecoflex-based TENG is biomechanical energy including human bending, walking, pressing which are mild excitations for TENGs [23,24]. However, harsh interaction forces including friction force, compression and even violent collision also exist during exercise and work which may lead to property loss and personal injury. With the rise of personal security awareness nowadays, it is imperative to develop multifunctional stretchable TENG with safeguarding and force sensing performance to further diversify TENGs and satisfy actual demand of utilizations.

Shear thickening fluid (STF) and shear stiffening gel (SSG) are a kind of smart material whose viscosity and storage modulus increase by orders of magnitude when the shear rate is beyond a critical value which shows promising applications in damping, vibration controlling, ballistic protection and body armors [25–28]. Overcoming the instability and fluidity of STF, SSG whose commercial name is silly putty, is more preferable in practical applications. It is in viscous state at rest and turns to rigidity once undergoing striking [29]. Due to the high viscosity and damping properties, various SSG-based functional materials and devices have been reported in recent years. A graphene/silly putty-based viscoelastic polymer showed high sensitivity to pressure which could be utilized as electromechanical sensor [30]. By mixing SSG with carbonyl iron particles, a multifunctional polymer composite with dual-stimuli-responsive properties have been fabricated [31]. A SSG-based sandwich panel could absorb about 75% of the kinetic energy in low-velocity impact which exhibited better properties of energy dissipation and stress distribution when comparing to the similar sandwich panels with chloroprene rubber cores and ethylene-propylene-diene monomer cores [32]. A smart SSG/Kevlar textile presented dramatic improvement of 190% in preventing and absorbing impact force with respecting to neat Kevlar fiber under dynamic impact excitation which presented safeguarding performance for human beings [33]. However, SSG is in viscoelastic state which could not sustain its shape. Introducing small amount of PDMS could improve the stability of SSG-based device [34]. To this end, SSG/PDMS with high damping capacity may provide an exciting way for multifunctional TENG to prevent and sensing external damages.

In this paper, a stretchable TENG with safeguarding and force-sensing properties have been developed based on shear stiffening gel/polydimethylsiloxane (SSG/PDMS) and GaInSn liquid metal. The storage modulus of SSG/PDMS is rate dependent which can change from 3.99 kPa to 0.16 MPa with the increase of shear frequency. Owing to triboelectrification and electrostatic induction, TENG can generate a maximum power of 182.17 μW, exhibiting a good energy-capturing property. The high stretchability also guarantees the flexible TENG collects ambient energy even with large tensile deformations. Additionally, it also possesses fast stimuli-responsive performance which enables to sense and monitor different human movements such as tapping, compression and finger bending. Finally, owing to the shear stiffening effect, TENG device can impede external collision by decreasing the impact force from 1687.37 N to 566.40 N as well as increasing the buffer time from 1.10 to 2.75 ms. The generated electrical data also distinguish various excitations even under harsh impact conditions.

2. Experimental sections

2.1. Materials and preparation of TENGs

Briefly, a mixture of boric acid and polydimethylsiloxane (with the mass ration of 2:15) was stirred and followed heated in over for 7 h. A solid SSG polymer gel could be obtained after cooling down the composite [31]. The hybrid SSG/PDMS was fabricated by using SSG, HTV silicone rubber (MVQ 110–2, bought from Dong Jue Fine Chemicals Nanjing Co., Ltd) and benzoyl peroxide with the mass ratio of 7: 3: 0.04 mixed by a two-roll miller. Then the hybrid polymer matrix was molded and cured in a metal mould under 20 MPa at 100 °C for 20 min (Fig. 1a, b). GaInSn liquid metal was then dipped dropwise on the groove (length, width and thickness: 30 × 30 × 1 mm) of SSG/PDMS matrix to form a conductive layer (Fig. 1c). After encapsulation and heat for several minutes, the GaInSn-based TENG was obtained.

2.2. Characterization systems

The rheological properties of the polymer composite were characterized by a commercial rheometer (Physica MCR 301, Anton Paar Co., Austria). The tested samples were molded into cylinder with the thickness of 1 mm and diameter of 2 cm. The tensile experiments were carried by MTS (Criterion 43, MTS System Co., America). SSG/PDMS and PDMS with the dimensions of 55 × 10 × 2 mm were stretched with different speeds. The compressing-releasing force was loaded by metal plate which was connected with an oscillator (HEV 500) and the triboelectric output performance of TENG were studied by a digital multi-meter (DMM6001). The impact tests were conducted by a drop hammer test system.

3. Result and discussion

3.1. Triboelectric performance of the liquid metal-based TENG

The preparation procedures of GaInSn-based TENG are shown in Fig. 1a-e. Fig. 1f is the applied GaInSn liquid metal. The PDMS (thickness of 3 mm) considered here is brittle which tends to break after stretched (Fig. S1). However, owing to the plasticity of shear stiffening gel [31], SSG/PDMS exhibits high elastic and stretchable property (Fig. 1g, h). The rheological properties of the polymer composites are studied (Fig. 1i). The storage modulus (G′) of PDMS is independent of shear frequency which the values at the frequencies of 0.1 and 100 Hz are 0.12 MPa and 0.11 MPa, respectively. However, SSG gel is soft which the initial G′ is 84.56 Pa (0.1 Hz) and it reaches 0.68 MPa when external shear frequency is 100 Hz which shows typical shear stiffening effect. Movie S1 also presents SSG is soft, stretchable but it also can protect human beings from the hammer impacts. As expected, the initial G′ value of SSG/PDMS is 3.99 kPa which shows soft and stretchable character (Fig. 1h). However, it increases to 0.16 MPa when the frequency is 100 Hz, presenting similar rate-dependent property. Thus, SSG/PDMS with shear stiffening effect shows great potential application in flexible wearable electronics. The electricity generation of this single-electrode mode TENG is mainly due to the coupling effect of triboelectrification and electrostatic induction which is schematically illustrated in Fig. 1j-m. When human skin contacts with SSG/PDMS of TENG, electrons can transfer from skin to the surface of TENG owing to their different electrification (Fig. 1j) [35]. As skin is moved, the negative charges stayed on the surface of SSG/PDMS will induce positive charges on GaInSn liquid metal to reach a new electrical equilibrium. On this occasion, the positive charges drive the free electrons to flow from the electrode to the ground, generating an output current signal (Fig. 1k). When human skin separates away, TENG will be electroneutral due to the balance of positive charges induced in the GaInSn liquid metal. Thus, no electron flow can be measured (Fig. 1l). Moreover, when skin moves back to TENG, the induced positive charges in the GaInSn will reduce, follow by the flow of free electron from the ground to liquid metal which forms a reversed electrical signal, as shown in Fig. 1m. To this end, continuous current output will be generated with cyclic compression-releasing processes.

Supplementary material related to this article can be found online at doi:10.1016/j.nanoen.2018.09.035

Kinetic energy with diverse amplitudes and frequencies are widespread in daily life. So it is essential to study the electric output performance of TENG under various excitations. Fig. 2a and b show the output voltage and current of TENG under different applied forces at a constant loading frequency of 5 Hz. The tested TENG with a size of $5 \times 5\ cm^2$ and thickness of 4 mm links with external resistance of 80 MΩ. Output voltage and current obviously increase in accordance with the increase of loading force. Especially, slight voltage signal of 4.20 V is generated under the force of 0.7 N, indicating the as-prepared TENG can harvest negligible motion energy (insert fig. in Fig. 2a). Voltage as well as current increase dramatically in the force range of 0.7–29 N and finally keep at 34.70 V and 0.43 μA, respectively (Fig. 2a, b; Fig. S2a, b). On the other hand, the frequency of constant contact-separation loading also shows positive influence on the output performance of TENG. For instance, voltages rise from 3.75 to 38.30 V as the loading frequencies vary from 0.5 to 10 Hz (Fig. 2c and Fig. S2c). Correspondingly, the currents change from 0.47 to 4.79 μA (Fig. 2d and Fig. S2d). This is mainly because high frequency of loading-unloading decrease the separation time and more generated charges accumulate on the electrode which results in higher current values [36–38]. Therefore, an appropriate loading force (27 N) and frequency (10 Hz)

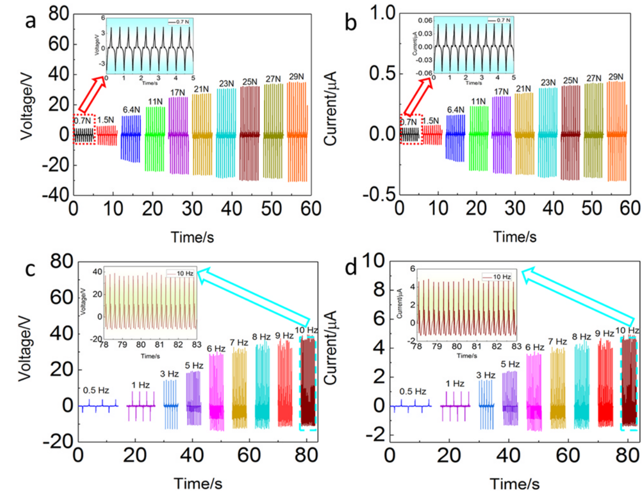

Fig. 2. Generated output voltage (a), current (b) of liquid metal-based TENG at 80 MΩ under various different applied forces; frequency dependent voltage (c), current (d) of TENG subjected to the force of 27 N under 8 MΩ loading resistance.

can lead to higher triboelectric output performance for GaInSn-based TENG.

Generally, external resistance is a significant influence on the electric performance of TENG. Therefore, establishing the relationship between power density and resistance is beneficial to practical applications. Thus, resistance (in the range of 1 kΩ–1 GΩ) dependent triboelectric outputs including voltage, current and power density were systematically investigated. As expected, voltage (black lines in Fig. 3a) of TENG (4 mm) is as low as 0.79 V under 100 kΩ. It starts to increase when the resistance is larger than 100 kΩ and finally reaches 70.33 V at the resistance of 1 GΩ. However, the maximum average current of TENG is 12.56 μA under the resistance of 1 kΩ and it keeps decreasing with the increase of external resistance due to the Ohm's law. The output power (calculated by $P = I^2R$) of TENG is presented in Fig. 3b. The maximum average power achieves 182.17 μW at the load resistance of 7 MΩ. The relative average voltage and current are 35.72 V and 5.10 μA which also show ideal stability (Fig. S3a, b). On the other hand, the triboelectric properties of GaInSn-based TENG with different thicknesses were also explored. Voltage of TENGs with 6 and 8 mm exhibit similar tendency to the values of TENG (4 mm) and the maximum average values are respective 53.50 V (Fig. 3c) and 42.41 V (Fig. 3e). The maximum load peak power of TENG with 6 mm is achieved at 109.00 μW across the 8 MΩ load resistance (output voltage and current are 29.54 V and 3.69 μA). As for TENG with 8 mm, an instantaneous peak power of 66.93 μW is obtained at 7 MΩ and the stable voltage and current are presented in Fig. S3c-f. According to the above results, the electric output properties of GaInSn-based TENG decrease with the increase of device thickness. Similar phenomena also exist in PDMS- [16,39], Kapton- [20,40] and PTFE-based TENG [41]. Although the thickness of SSG/PDMS polymer is much thicker than the dielectric layers of the reported TENGs (micron levels), the mechanism can also be used to explain our results. According to the calculations in previous works [42–45], the thicker SSG/PDMS layer impedes the agglomeration of triboelectric charges owing to the higher dielectric constant which in turn decreases the output voltage. On the other hand, more kinetic energy will be absorbed and dissipated by thicker SSG/PDMS polymer (if assuming SSG/PDMS is a linear elastic body, thicker polymer has a higher spring coefficient). Thus, the actual force loading on TENG declines which leads to a decreasing triboelectric charges and lower output voltage. The stability of TENG with 4 and 6 mm are also explored and presented in Fig. 3g and h. Clearly, the ideal output voltage signals over 3000 loading-unloading motions show no degradation

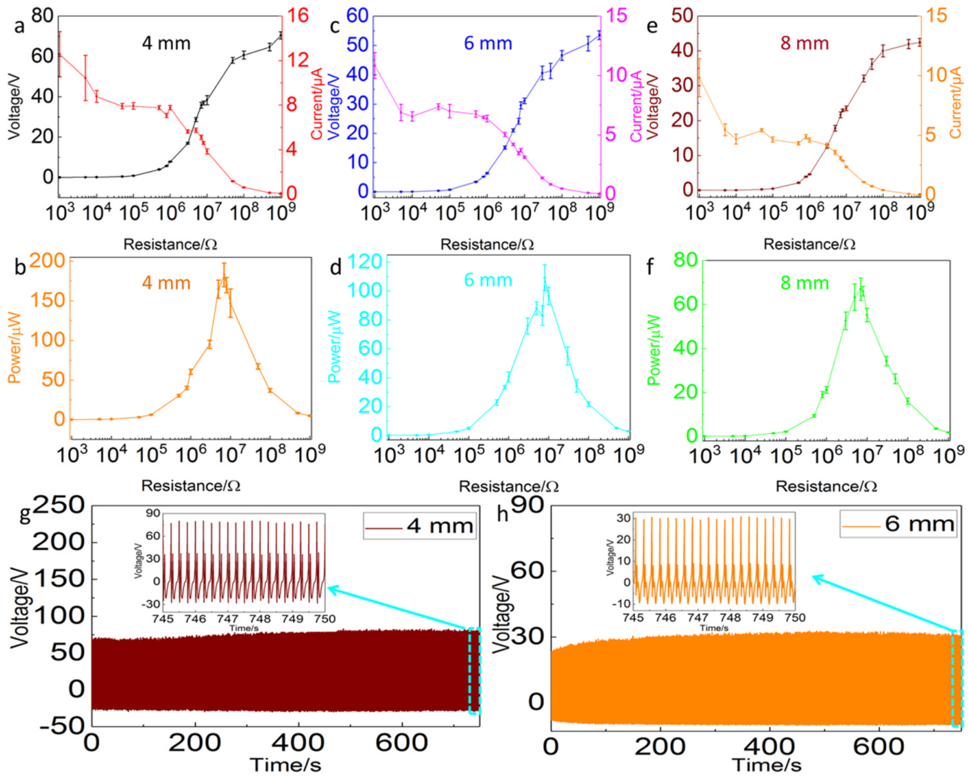

Fig. 3. Thickness dependent of TENG subjected to 27 N at a frequency of 10 Hz with different external resistance: electric voltage, current and power output of 4 (a, b), 6 (c, d) and 8 (e, f) mm; Stability of TENG with 4 (g) and 6 (h) mm at 500 MΩ.

owing to the ideal durability of SSG/PDMS polymer matrix. Therefore, TENG with 4 mm is more desirable as a wearable power source for practical applications.

3.2. Output properties of TENG under different tensile elongations

The triboelectric performance of TENG under different elongations was evaluated to mimic its practical working conditions. Originated from the good elasticity and stretchability of SSG, the configuration of the fabricated TENG can maintain stable even under extreme deformation (Fig. 4a, b). The tensile forces of SSG/PDMS with the sizes of 5.5 × 1 cm and thickness of 2 mm under different stretching speeds were measured. Clearly, the maximum force increase from 0.96 to 4.58 N in the stretching speeds of 10–500 mm/min, indicating a typical rate-dependent effect. The maximum strain of SSG/PDMS can reach 187% when stretching with 500 mm/min. As for PDMS, the increase of maximum force under different stretching speeds is not obvious (Fig. S4). Triboelectric current and the corresponding power of TENG with various loading resistance at the stretch ratio of 20% are presented in Fig. 4g and j. Output current signals are very stable with different resistance during cycles of contact-separation processes and they undoubtedly decrease with the increase of load resistance. However, the triboelectric output performance all increase when compared with pristine TENGs. For example, current and power of TENG in initial state are 5.73 μA and 164.48 μW while they respectively increase to 6.70 μA and 224.34 μW when TENG is stretched to 20% at 5 MΩ. To prove the feasibility of stretched TENG as a power resource, an array of LEDs is connected with the nanogenerator. They can work effectively without any power unit which demonstrates stretched TENG enables to harvest mechanical energy from ambient environment (Fig. 4d-f). This increment is due to the coupling effect of contact surface areas and thickness of SSG/PDMS layers. Owing to the Poisson's effect, the thickness of SSG/PDMS decreases when stretched and the thinner dielectric layer enables to increase the amount of induced charges in the GaInSn liquid metal during contact-separation process [19,20]. At the same time, the increased contacting area after stretched is also favorable to the transformation of electrons. Thus the total triboelectric output performance is increased. Current and power density of TENG with the axial deformation of 60% show similar increasing tendency (Fig. 4h and k). The stretch ratio dependent current and power under 7 MΩ were further studied. The surface contacting area of TENG is increased after stretching. As expected, the energy-harvesting performance is increased as current vary from 5.10 to 6.80 μA during the stretch ration of 0–80% and the corresponding power output also increase from 182.17 to 323.97 μW. To this end, the GaInSn-based TENG with high tensile strain and outstanding triboelectric output in the lateral stretching mode ensures it as a deformable self-power electronics.

3.3. Self-powered mechanosensing properties of the TENG device

Taking advantage of the high stretchability, flexibility and good sensitivity of TENG (4 mm), the device can act as a self-powered sensor used for physiological monitoring. Firstly, TENG is attached on human arm and different nitrile-gloved fingers (from 1 to 4) slight stroke are subjected (Fig. 5a). Interestingly, TENG can feel the excitation by changing voltage from 0.59 V (induced by stroke of 1 finger) to 1.15 V (4 fingers) and finally it exhibits good recovery property which the voltage decrease to 0.65 V (2 fingers). TENG also can detect different pressures generated by nitrile-gloved fingers tapping with changing the distinguished voltage signals (Fig. 5b). Additionally, TENG fixed on human hand monitors the bending-releasing behaviors with repeated cycles (Fig. 5c). According to the triboelectric series, the working mechanism of TENG during bending process is mainly because of the contact-induced electrification and the changes of generated charges caused by the relative sliding between fingers and TENG surface [46]. Besides sensing normal physiological motions, the as-prepared TENG can also act as a proof-of-concept force sensor to detect the impact of various hammers which is more important in harsh collisions (Fig. 5d).

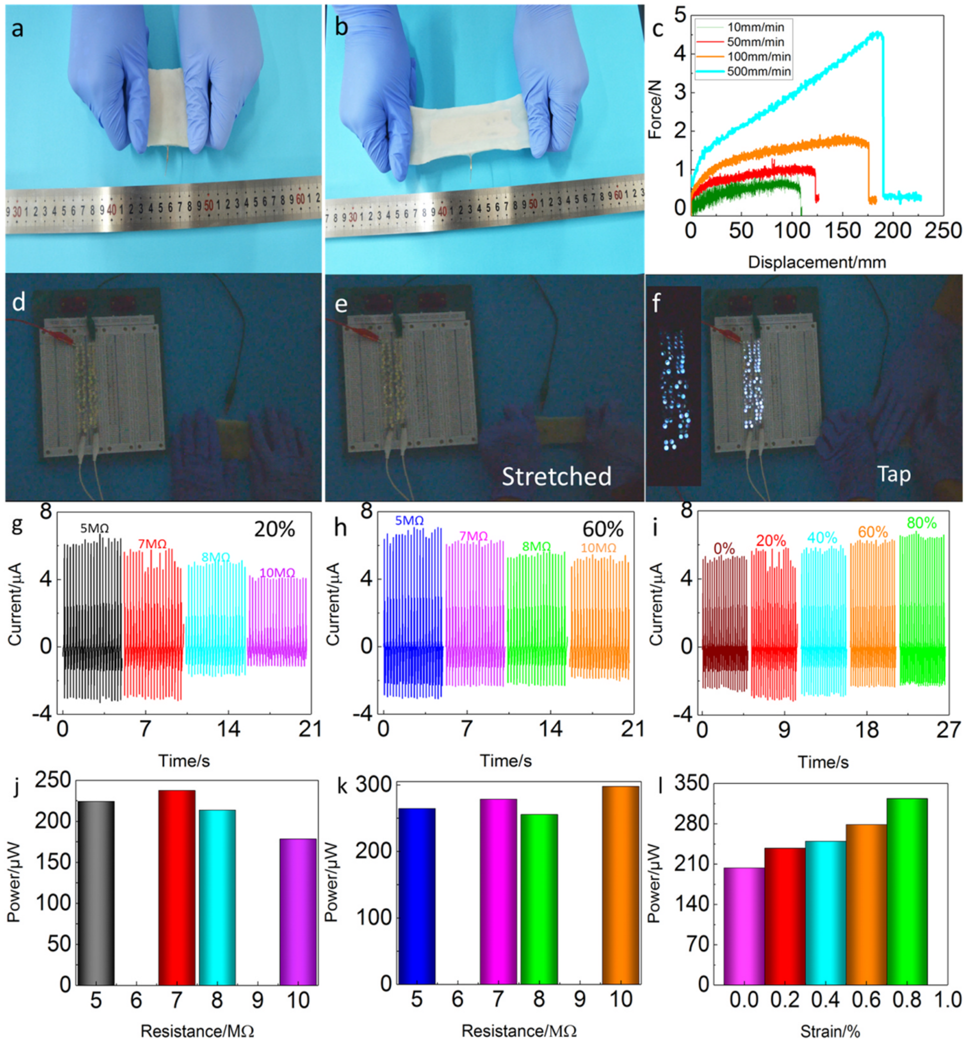

Fig. 4. The elongation of GaInSn-based TENG (a, b); tensile force-displacement curves of SSG/PDMS with different speeds (c); a tensile TENG can harvest mechanic energy to electric energy and light up LEDs (d-f); triboelectric current and power output under different load resistance with tensile strain at 20% (g, j) and 60% (h, k), respectively; current (i) and power output (l) of TENG at 7 MΩ resistance with elongation strain ranging from 0–80%.

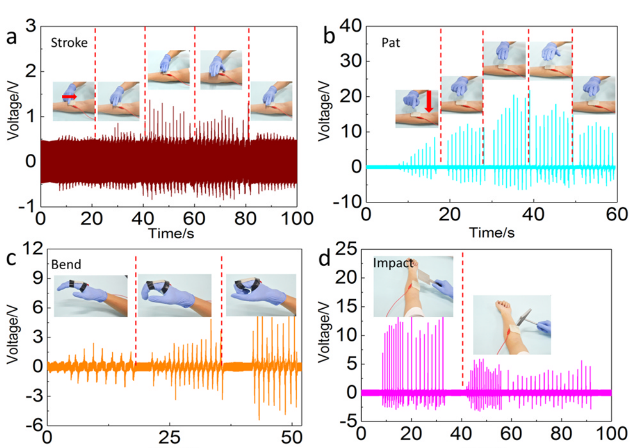

Fig. 5. Photographs and self-powered force sensing of TENG to monitor: finger stroking (a) and tapping (b), human hand bending/relaxation (c), impact at different loading speeds by two hammers with different shapes (d).

An elevated voltage at 13.66 V is due to the impact of a metal plate with flat head while it decreases to 5.92 V when a hammer strikes on TENG. Simultaneously, the responsive voltage signals are in accordance with the impact frequency which also demonstrates its fast response to stimuli. In conclusion, GaInSn-based TENG with high flexibility, sensitivity and rapid response can not only harvest energy as a self-powered system but also detect and monitor a variety of physiological motions ranging from gentle touch to large bending deformation which have potential application in developing multifunctional wearable electronics for medical diagnosis and human-machine interactive devices.

3.4. Force sensing and safeguarding properties of TENG

In consideration of the energy dissipation effect of SSG/PDMS, the anti-impact as well as the triboelectric performance of TENG were systematically investigated. A drop harmer test device connected with force sensor, digital multi-meter, charge amplifier and oscilloscope were used to study the self-powered sensing and safeguarding properties of TENG. The systems were provided in Fig. S5. The as-prepared TENG devices were $5 \times 5\,cm^2$ and the thickness changed from 4 to

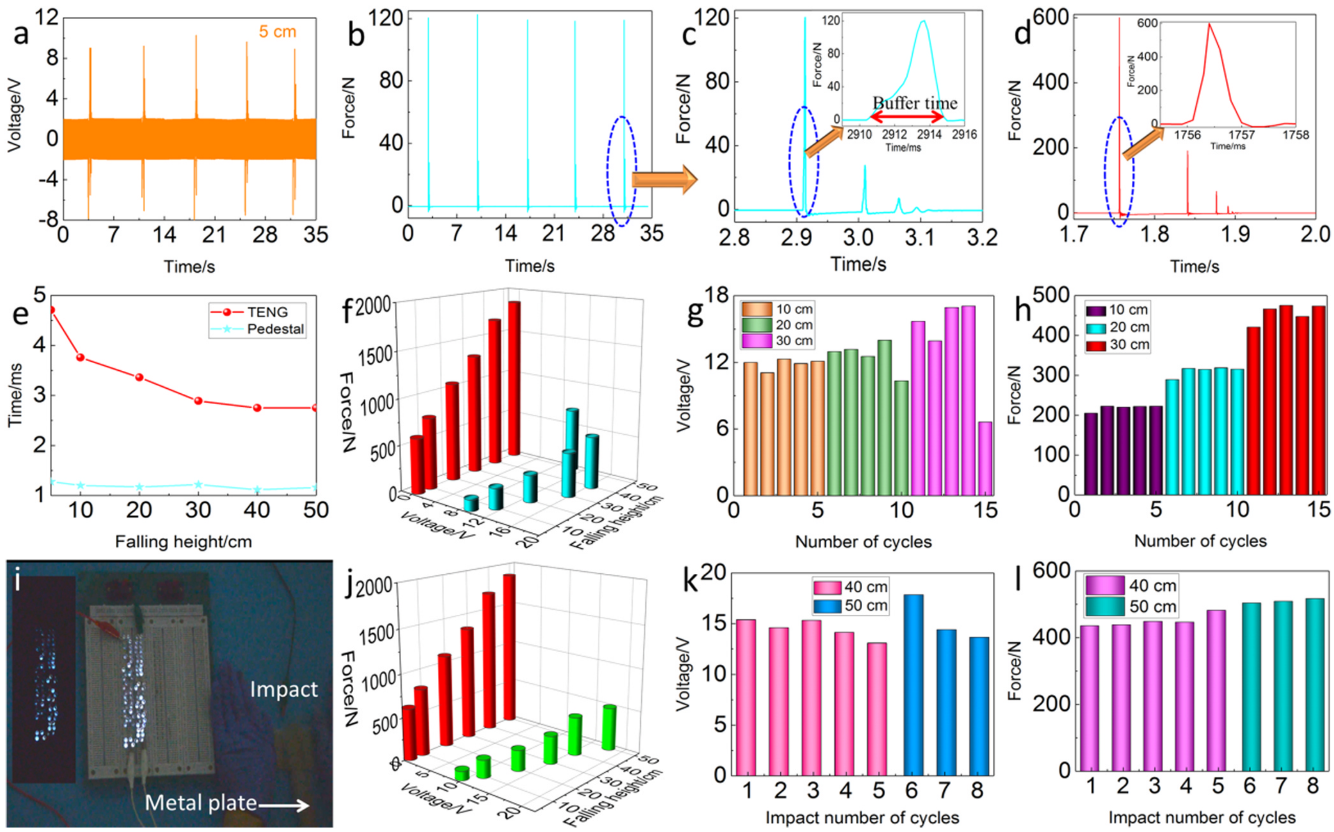

Fig. 6. Demonstration of GaInSn-based TENG as a self-powered force sensor with safeguarding performance. Output voltage (a) and impact force (b) signals of TENG (4 mm) generated by the impact from 5 cm, typical force-time curves impacted on TENG (c), metal force sensor (d) and the corresponding buffer times (e), voltage and impact force vs falling heights in the range of 5–50 cm (The red bars represent the signals loaded on force sensor) (f), cyclic stability of output voltage (g) and loading force (h) of TENG, power LEDs by impacting a stretchable TNEG (4 mm) using metal plate (i); impact force and voltage of TENG (6 mm) versus falling heights in the range of 5–50 cm (j), cyclic stability of voltage (k) and loading force (l) of TENG (6 mm) from the impact of 40 and 50 cm.

6 mm. Once loaded by the impactor from 5 cm, a voltage peak value of 9.2 V can be observed which is due to the triboelectric effect (Fig. 6a). The impact force recorded by the force sensor increase sharply once contacts TENG and after reaching a maximum value it decreases to initial value (Fig. 6c). Additionally, the impactor damps for several times which can dissipate much strike energy. When comparing with the maximum force loading directly on metal force sensor (Fig. 6d), it decreases from 596.31 to 120.43 N which implies the TENG can dissipate 79.81% of impact energy and provide favorable protection. The stable impact forces presented in Fig. 6b also demonstrate TENG (4 mm) can sustain the external excitation and simultaneously output reliable voltage signals. The buffer times loaded on TENG device and force sensor are also studied. The largest time is 4.71 ms once the falling height is 5 cm and it decreases with increase of falling heights and finally balances at 2.75 ms as the falling height reaches 40 cm. However, the buffer time generated by the impact on metal force sensor is about 1.1 ms which is independent of falling heights. The dramatic improvement in buffer time also demonstrates the TENG device with SSG/PDMS remarkably enables to impede external impact and act as protective material for safeguards. Output voltage, impact force of TENG (4 mm) versus falling heights are shown in Fig. 6f. Voltage increases from 9.02 to 16.29 V with the falling heights rising from 5 to 40 cm. These distinguished voltage signals can be used to monitor external impact excitations. Simultaneously, the impact force display the similar tendency which it increases from 120.43 to 566.40 N. Comparing with the forces loaded directly on the force sensor, TENG can dissipate much impact energy which provides favorable protection effect. For example, keeping the falling height at 40 cm, the impact force directly on the sensor is as high as 1687.37 N while it dramatically reduces to 566.40 N if loaded on the TENG device (decreased by 66.43%). And the forces loaded directly on force sensor elevate from 600.02 to 1687.37 N with the falling heights of 5–40 cm. The remarkable reduction of impact force implies TENG can dissipate kinetic energy thus protect human beings. Fig. 6g is the voltage cyclic stability of TENG dropped from 10 to 30 cm. Clearly, TENG is capable of resisting external impact and outputting stable voltages in 5 loading-unloading excitations. However, micro-cracks appear owing to the continuous impact from 30 cm and GnInSn permeate into SSG/PDMS which leads to a decrease of voltage from 17.07 to 6.63 V while the impact forces keep stable (Fig. 6h) which proves the reduction of safeguarding performance of TENG is negligible after cyclic impact loadings. A total of 80 LED bulbs are directly powered even by the impact of metal plate on a stretched TENG (Fig. 6i and Movie S2). When the falling height is higher than 40 cm, SSG/PDMS destroys and GaInSn flows out which voltage decrease dramatically (Fig. S6a). However, the anti-impact force is stable even the falling height reaches 50 cm (Fig. S6b). In comparison, falling height dependent electric and mechanic properties of GaInSn-based TENG (6 mm) are also exhibited in Fig. 6j. Output voltage as well as the force signals show similar tendency when compared with those in Fig. 6f. Undoubtedly, TENG (6 mm) demonstrates better anti-impact performance under the same excitation. For instance, the loading force of TENG (6 mm) is 447 N when the falling height is 40 cm which decreases by 21% than the force of TENG (4 mm). Due to the increased thickness, the impact force (Fig. 6l) and voltage output (Fig. 6k) of TENG (6 mm) are stable when the falling height is larger than 40 cm. Thus, the fabricated GaInSn-based TENG could be applied as a smart

self-powered force sensors as well as a safeguarding protector for next generation wearable portable devices.

Supplementary material related to this article can be found online at doi:10.1016/j.nanoen.2018.09.035

4. Conclusion

In summary, a self-powered multifunctional triboelectric nanogenerator with protecting and sensing properties has been designed by injecting GaInSn liquid metal into SSG/PDMS matrix. The TENG device with optimized thickness of 4 mm shows high efficiency of gathering mechanical energy with current of 5.10 μA, and an output power of 182.17 μW. Moreover, the as-prepared TENG exhibits enhanced triboelectric current and power even stretched to 80%. The nanogenerator acted as a self-powered sensor also shows multiple sensing performance which can monitor various physiological excitations. Benefited from the shear stiffening effect, TENG device with 4 mm can sustain and impede continuous collisions and decrease the impact force from 1687.37 N to 566.40 N. Thus, the reliable multifunction of the liquid metal-based TENG ensure its practical utilization in wearable electronics, green energy sources and safeguards.

Acknowledgments

Financial supports from the National Natural Science Foundation of China (Grant No. 11772320, 11802303), the Strategic Priority Research Program of the Chinese Academy of Sciences (Grant No. XDB22040502), the Fundamental Research Fund for the Central Universities (WK2090050045) and China Postdoctoral Science Foundation (Grant No. 2018M632543) are gratefully acknowledged. This study was also supported by the Collaborative Innovation Center of Suzhou Nano Science and Technology and partially carried out at the USTC Center for Micro and Nanoscale Research and Fabrication.

Appendix A. Supporting information

Supplementary data associated with this article can be found in the online version at doi:10.1016/j.nanoen.2018.09.035.

References

[1] T. Someya, Z.N. Bao, G.G. Malliaras, Nature 540 (2016) 379–385.
[2] W.Z. Wu, L. Wang, Y.L. Li, F. Zhang, L. Lin, S.M. Niu, D. Chenet, X. Zhang, Y.F. Hao, T.F. Heinz, J. Hone, Z.L. Wang, Nature 514 (2014) 470–474.
[3] M.Y. Shi, J.X. Zhang, H.T. Chen, M.D. Han, S.A. Shankaregowda, Z.M. Su, B. Meng, X.L. Cheng, H.X. Zhang, ACS Nano 10 (2016) 4083–4091.
[4] C.G. Núñez, W.T. Navaraj, E.O. Polat, R. Dahiya, Adv. Funct. Mater. 27 (2017) 1606287–1606299.
[5] K.C. Chan, L.H. Hee, O.K. Hwan, S.J. Yun, Science 535 (2016) 682–687.
[6] Y.C. Ding, W.H. Xu, W.Y. Wang, H. Fong, Z.T. Zhu, ACS Appl. Mater. Interfaces 9 (2017) 30014–30023.
[7] F.R. Fan, Z.Q. Tian, Z.L. Wang, Nano Energy 1 (2012) 328–334.
[8] Z.L. Wang, ACS Nano 7 (2013) 9533–9557.
[9] X.H. Yu, J. Pan, J. Zhang, H. Sun, S.S. He, L.B. Qiu, H.Q. Lou, X.M. Sun, H.S. Peng, J. Mater. Chem. A 5 (2017) 6032–6038.
[10] C.M. Cui, X.Z. Wang, Z.R. Yi, B. Yang, X.L. Wang, X. Chen, J.Q. Liu, C.S. Yang, ACS Appl. Mater. Interfaces 10 (2018) 3652–3659.
[11] X.X. Chen, Y. Song, H.T. Chen, J.X. Zhang, H.X. Zhang, J. Mater. Chem. A 5 (2017) 12361–12369.
[12] Y.J. Su, G.Z. Xie, F.B. Xie, T. Xie, Q.P. Zhang, H.L. Zhang, H.F. Du, X.S. Du, Y.D. Jiang, Chem. Phys. Lett. 653 (2016) 96–100.
[13] H.L. Zhang, Y. Yang, Y.J. Su, J. Chen, K. Adams, S. Lee, C.G. Hu, Z.L. Wang, Adv. Funct. Mater. 24 (2014) 1401–1407.
[14] S.H. Shin, Y.H. Kwon, Y.H. Kim, J.Y. Jung, J. Nah, Nanomaterials 6 (2016) 186–194.
[15] X. Pu, M.M. Liu, X.Y. Chen, J.M. Sun, C.H. Du, Y. Zhang, J.Y. Zhai, W.G. Hu, Z.L. Wang, Sci. Adv. 3 (2017) 1700015–1700026.
[16] T.C. Lai, J.N. Deng, S.M. Niu, W.B. Peng, C.S. Wu, R.Y. Liu, Z. Wen, Z.L. Wang, Adv. Mater. 28 (2016) 10024–10032.
[17] J.N. Deng, X. Kuang, R.Y. Liu, W.B. Ding, A.C. Wang, Y.C. Lai, K. Dong, Z. Wen, Y.X. Wang, L.L. Wang, J.H. Qi, T. Zhang, Z.L. Wang, Adv. Mater. 30 (2018) 1705918–1705928.
[18] X. Wang, Y. Yin, F. Yi, K. Dai, S. Niu, Y. Han, Y. Zhang, Z. You, Nano Energy 39 (2017) 429–436.
[19] H. Guo, M.H. Yeh, Y.C. Lai, Y.L. Zi, C.S. Wu, Z. Wen, C.G. Hu, Z.L. Wang, ACS Nano 10 (2016) 10580–10588.
[20] W. Tang, T. Jiang, F.R. Fan, A.F. Yu, C. Zhang, X. Cao, Z.L. Wang, Adv. Funct. Mater. 25 (2015) 3718–3725.
[21] L.E. Helseth, Nano Energy 50 (2018) 266–272.
[22] H. Wu, Q. Shi, F. Wang, A.V. Thean, C. Lee, Small Methods 2 (2018) 1800078–1800087.
[23] Y.J. Fan, X.S. Meng, H.Y. Li, S.Y. Kuang, L. Zhang, Y. Wu, Z.L. Wang, G. Zhu, Adv. Mater. 29 (2017) 1603115–1603123.
[24] T.X. Xiao, T. Jiang, J.X. Zhu, X. Liang, L. Xu, J.J. Shao, C.L. Zhang, J. Wang, Z.L. Wang, ACS Appl. Mater. Interfaces 10 (2018) 3616–3623.
[25] I.R. Peters, S. Majumdar, H.M. Jaeger, Nature 532 (2016) 214–217.
[26] T.F. Tian, M. Nakano, Smart Mater. Struct. 26 (2017) 035038–035045.
[27] C.H. Xu, Y. Wang, J. Wu, S.C. Song, S.S. Cao, S.H. Xuan, W.Q. Jiang, X.L. Gong, Comp. Sci. Technol. 153 (2017) 168–177.
[28] E.E. Haro, A.G. Odeshi, J.A. Szpunar, Int. J. Impact Eng. 96 (2016) 11–22.
[29] W.F. Jiang, X.L. Gong, S. Wang, Q. Chen, H. Zhou, W.Q. Jiang, S. Hu. Xuan, Appl. Phys. Lett. 104 (12) (2014) 121915–121920.
[30] C.S. Boland, U. Khan, G. Ryan, S. Barwich, R. Charifou, A. Harvey, C. Backes, Z.L. Li, M.S. Ferreira, M.E. Möbius, R.J. Young, J.N. Coleman, Science 354 (2016) 1257–1260.
[31] S. Wang, W.Q. Jiang, W.F. Jiang, F. Ye, Y. Mao, S.H. Xuan, X.L. Gong, J. Mater. Chem. C 2 (34) (2014) 7133–7140.
[32] Y.P. Wang, X.L. Gong, S.H. Xuan, Smart Mater. Struct. 27 (2018) 065008–065012.
[33] S. Wang, S.H. Xuan, M. Liu, L.F. Bai, S.S. Zhang, M. Sang, W.Q. Jiang, X.L. Gong, Soft Matter 13 (2017) 2482–2491.
[34] S. Wang, L.P. Gong, Z.J. Shang, L. Ding, G.S. Yin, W.Q. Jiang, S.H. Xuan, Adv. Funct. Mater. 28 (2018) 1707538–1707547.
[35] Y.Q. Yang, N. Sun, Z. Wen, P. Cheng, H.C. Zheng, H.Y. Shao, Y.J. Xia, C. Chen, H.W. Lan, X.K. Xie, C.J. Zhou, J. Zhong, X.H. Sun, S.T. Lee, ACS Nano 12 (2018) 2027–2034.
[36] Z.M. Tian, J. He, X. Chen, Z.X. Zhang, T. Wen, C. Zhai, J.Q. Han, J.L. Mu, X.J. Hou, X.J. Chou, C.Y. Xue, Nano Energy 39 (2017) 562–570.
[37] C.W. Xu, L. Zhang, Y.L. Xu, Z.Z. Yin, Q. Chen, S.Y. Ma, H.H. Zhang, R. Huang, C.L. Zhang, L. Jin, W.Q. Yang, J. Lu, J. Mater. Chem. A 5 (2017) 189–201.
[38] H.J. Kim, J.H. Kim, K.W. Jun, J.H. Kim, W.C. Seung, O.H. Kwon, J.Y. Park, S.W. Kim, I.K. Oh, Adv. Energy Mater. 6 (2016) 1502329–1502335.
[39] X.B. Chen, Q. Xu, S. Bai, Y. Qin, Nano Energy 33 (2017) 288–292.
[40] M.Y. Ma, Z. Zhang, Q.L. Liao, G.J. Zhang, F.F. Gao, X. Zhao, Q. Zhang, X.C. Xun, Z.M. Zhang, Y. Zhang, Nano Energy 39 (2017) 524–531.
[41] G. Zhu, Y.S. Zhou, P. Bai, X.S. Meng, Q.S. Jing, J. Chen, Z.L. Wang, Adv. Mater. 26 (2014) 3788–3796.
[42] S. Niu, Y. Liu, X. Chen, S. Wang, Y.S. Zhou, L. Lin, Z.L. Wang, Nano Energy 12 (2014) 760–774.
[43] F. Yi, X.F. Wang, S.M. Niu, S.M. Li, Y.J. Yin, K.R. Dai, G.J. Zhang, L. Lin, Z. Wen, H.Y. Guo, J. Wang, M.H. Yeh, Y.L. Zi, Q.L. Liao, Z. You, Y. Zhang, Z.L. Wang, Sci. Adv. 2 (2016) 1501624–1501634.
[44] H.Y. Qiao, Y. Zhang, Z.G. Huang, Y.M. Wang, D.Q. Li, H.M. Zhou, Nano Energy 50 (2018) 126–132.
[45] P. Kaushik, K. Vipin, J.X. Wang, B. Venkateswarlu, B. Ramaraju, S.L. Pooi, Adv. Mater. 29 (2017) 1702181–1702189.
[46] Y.F. Li, G. Cheng, Z.H. Lin, J. Yang, L. Lin, Z.L. Wang, Nano Energy 11 (2015) 323–332.

Sheng Wang received his Ph.D. degree from University of Science and Technology of China in 2017. Now he is a postdoctoral fellow in the Chinese Academy of Sciences Key Laboratory of Mechanical Behavior and Design of Materials in Hefei, China. His research interests include smart materials and devices with magnetic, electric and force-sensing properties. He is also currently interested in developing multifunctional triboelectric nanogenerator systems.

Li Ding received her B.S. degree in Astronautic Engineering and Mechanics from Harbin Institute of Technology, Harbin, Heilongjiang, P.R. China in 2015. She is currently a Ph.D. candidate in Department of Modern Mechanics at University of Science and Technology of China. Her research interests are focused on smart sensing materials and magnetically controllable devices.

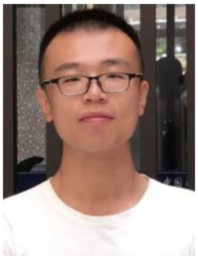

Xiwen Fan received his Bachelor degree from the University of Science and Technology of China and continued his research under the direction of Prof. Xinglong Gong in the Intelligent Materials and Vibration Control Laboratory. His research focuses on the mechanical properties of soft materials and the application of bio-inspired multifunctional composite.

Wanquan Jiang is an Associate Professor in the Department of Chemistry, USTC, China. He received his B.Sc. from Anhui University in 1984 and Ph.D. from USTC in 2002. After graduation, he also worked as a postdoctoral fellow in National Taiwan University for 1 year. Dr. Jiang's research interests include synthesis and characterization of advanced smart materials with magnetic, electric responsive properties for sensing and damping applications.

Xinglong Gong received his Ph.D. degree in Mechanics from both the University of Science and Technology of China (USTC, China) and Saitama University (Japan), in 1996. Then, he worked at the Nihon Dempa Kogyo Co., Ltd., Japan. In 2003, he joined the Department of Modern Mechanics, USTC, as a Full Professor. He is currently the council chairman of Chinese Society of Experimental Mechanics. His research interests comprise soft matter materials as well as their applications. He was supported by the 100-Talent Programme of Chinese Academy of Sciences in 2003 and supported by the National Science Foundation for Distinguished Young Scholars of China in 2011.